Evolution of the Nankai Trough décollement from the trench into the seismogenic zone: Inferences from three-dimensional seismic reflection imaging

Nathan L. Bangs
Thomas H. Shipley
Sean P.S. Gulick
Institute for Geophysics, University of Texas, 4412 Spicewood Springs Road, Austin, Texas 78759, USA
Gregory F. Moore Department of Geology and Geophysics, University of Hawaii at Manoa, Honolulu, Hawaii 96822, USA
Shinichi Kuromoto Center for Deep Earth Exploration, Japan Marine Science and Technology Center, 2-15, Natsushima-cho, Yokohama, Kanagawa 237-0061, Japan
Yasuyuki Nakamura Ocean Research Institute, University of Tokyo, 1-15-1 Minamidai, Nakano-ku, Tokyo 164-8639, Japan

ABSTRACT

We mapped the amplitude of the Nankai Trough subduction thrust seismic reflection from the trench into the seismogenic zone with three-dimensional seismic reflection data. The décollement thrust forms within the lithologically homogeneous Lower Shikoku Basin facies along an initially nonreflective interface. The reflection develops from a porosity contrast between accreted and underthrust sedimentary material because of accretionary wedge consolidation and rapid loading and delayed consolidation of the underthrust section. A décollement-amplitude map shows a significant decline from high amplitudes at the trench to barely detectable levels 25–30 km landward. Three other observations coincide with the amplitude decline: (1) the décollement initially steps down to deeper stratigraphic levels, (2) the wedge taper increases dramatically, and (3) the thrust becomes seismogenic. The amplitude decline and the coincident décollement and accretionary-wedge tectonic and seismogenic behavior are attributed to the loss of fluids and potentially loss of excess fluid pressures downdip along the subduction thrust.

Keywords: subduction zone, accretionary wedge, seismogenic zone, décollement, pore fluid, faults.

INTRODUCTION

Numerous observations show that subduction-related plate-boundary faults are inherently weak (Davis et al., 1983), fluid rich (Shipley et al., 1994; Bangs et al., 1999), and aseismic (Byrne et al., 1988) along their updip parts beneath accretionary wedges. However, subduction-zone thrusts produce some of the world's largest and most devastating earthquakes, implying significant downdip transformation of properties from the trench into the seismogenic zone. Although clay-mineral transformation has been attributed to the onset of seismogenesis (Hyndman et al., 1995), even margins with small amounts of smectite show characteristic aseismic-to-seismic transitions. Moore and Saffer (2001) attributed other diagenetic, metamorphic, and consolidation processes to fluid sources that maintain high porosity and pore-fluid pressure along the aseismic parts of the subduction thrust and ultimately determine the updip limit of the seismogenic zone. Despite the potential significance of consolidation and fluid pressure in controlling stick-slip behavior and seismic rupture (Marone, 1998; Scholz, 1998), the relationship between fluids and seismicity stems from inferred diagenetic reactions and hydrogeologic models (Moore and Saffer, 2001; Saffer and Bekins, 1998), but there are few observations. We map the seismic reflections of the décollement over an unprecedented extent to infer how deep the fluid-rich fault extends and how consolidation of the décollement and subjacent rocks affects structure, tectonics, and especially seismicity in the Nankai Trough subduction zone.

ASEISMIC-TO-SEISMIC TRANSITION OFF SOUTHEAST SHIKOKU

The 1946 Nankaido M 8.0 event is the most recent of a regular series of major earthquakes off Shikoku Island. Nankaido coseismic rupture inferred from inversions of tsunami and geodetic data (Ando, 1982) extends updip to ~4 km subseafloor and <40 km from the trench (Fig. 1). Analysis of the tsunami data locates the rupture primarily at the downdip end of the seismogenic zone (Fig. 1) (Tanioka and Satake, 2001), linked to seamount subduction (Kodaira et al., 2000); only small displacement (<1 m) occurred at the updip end. Microseismicity also increases significantly between 30 and 40 km from the trench (Obana et al., 2003), and coincides (within 10 km) with the inferred updip limit of coseismic rupture of the Nankaido event (Figs. 1 and 2[1]). The thermally controlled interseismic locked zone of Hyndman et al. (1995) defines the updip limit of the aseismic-to-seismic transition as coinciding with the 150 °C isotherm, which is shallow along the Muroto transect because of the young (ca. 16 Ma) age of the subducting oceanic crust (Okino and Kato, 1995). The interseismic locked zone extends updip 4 km subseafloor and ~35 km landward from the trench, coincident with the updip extent of microseismicity. We interpret this limit as a transition to significantly greater stick-slip behavior along the subduction thrust, which was the target of our three-dimensional seismic survey.

THREE-DIMENSIONAL SEISMIC REFLECTION DATA

Acquisition and Processing

We designed the seismic survey to image the subduction thrust from the trench into the seismogenic zone (Fig. 1). Accurate images of the décollement to map its reflection amplitude beneath the complex accretionary-wedge structure require a dense array of long-offset three-dimensional seismic reflection data and computationally and labor-intensive processing. We acquired 81 lines, each 80 km long, with a single streamer on the R/V *Ewing* in 1999. The lines are 100 m apart and thus cover an 8 × 80 km^2 area (Fig. 1). We used a Racal differential global positioning system (GPS) navigational system for determining ship's position, shot spacing, and tail-buoy location. The seismic source was a tuned 14 airgun, 70 L (4273 in^3) array with sizes from 1.3 to 10.5 L (80–640 in^3). This source is capable of resolving layers ~10–12 m thickness. The receiver array was the R/V *Ewing's* Syntrac 6000 m streamer with 240 channels at 25 m spacing. Data were recorded at 2 ms sampling for 12 s. Streamer depth was maintained with

[1]Loose insert. Figure 2. Seismic line 300 and map of décollement-reflection amplitude across 8 × 50 km^2 area.

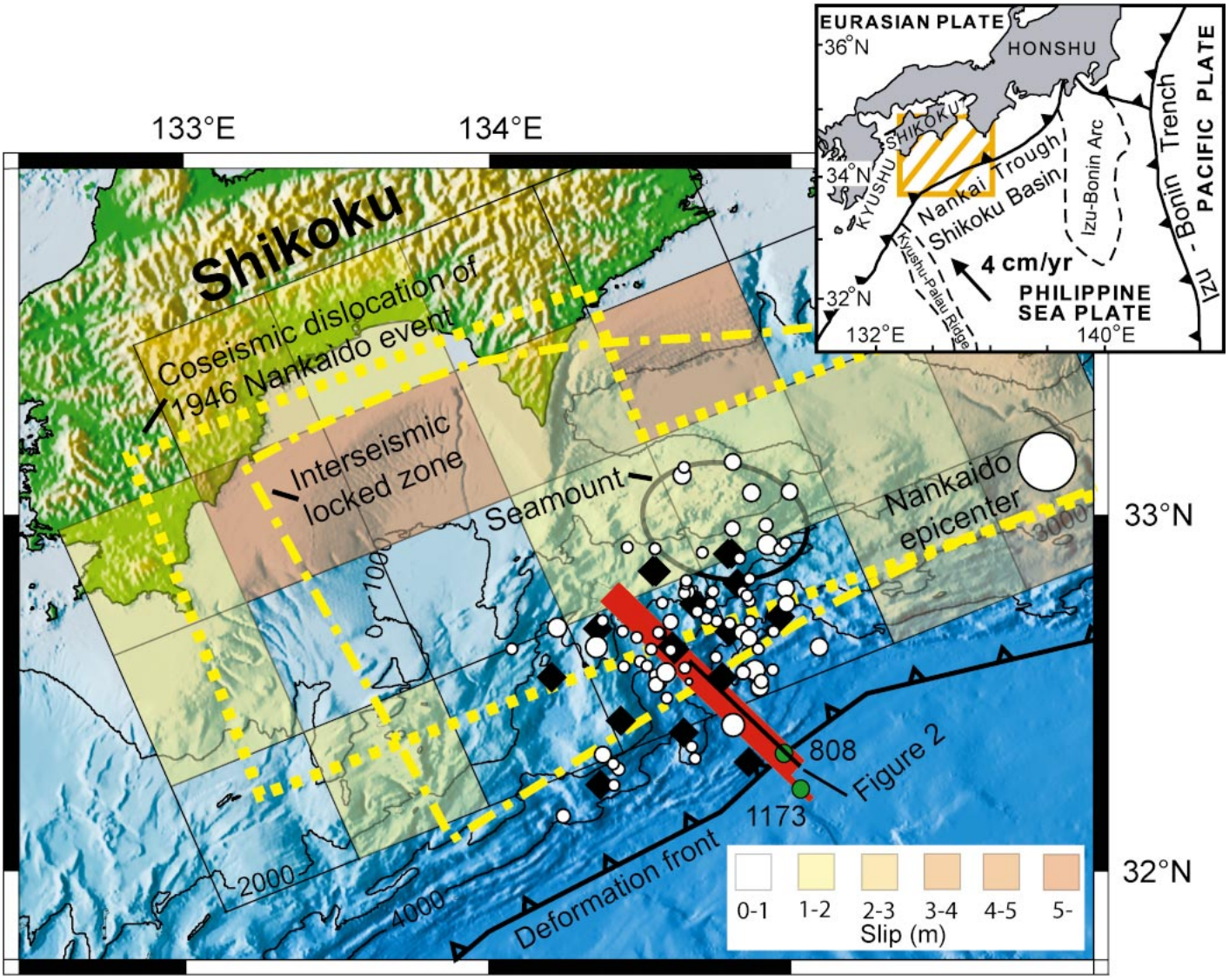

Figure 1. Location map showing three-dimensional seismic reflection survey area (red) and its relationship to updip limit of seismogenic zone. Bathymetry is in meters. Small white circles are locations of microseismicity epicenters recorded on ocean-bottom seismometer receivers (black diamonds) (Obana et al., 2003). Size indicates relative magnitude. Dot-dashed line indicates seismic locked zone defined by Hyndman et al. (1995). Short dashed line is coseismic rupture area of 1946 Nankaido event defined by Ando (1975). Colored squares are slip areas and magnitudes of Nankaido event by Tanioka and Satake (2001). Subducted seamount location is from Kodaira et al. (2000). Green dots mark Ocean Drilling Program Sites 808 and 1173.

control birds every 300 m and position reconstructed from 11 compasses spaced at 600 m and some tail-buoy differential GPS data.

We constructed three-dimensional seismic images of the volume with three-dimensional prestack time migration (Fig. 2A), which is unprecedented in academic marine seismic imaging. The best images of the décollement resulted when (1) each of the $\sim 34 \times 10^6$ traces was individually migrated in three dimensions by using Kirchhoff prestack time migration with the Geodepth processing software package and (2) migrated traces common to 50×25 m bins were stacked into an image volume of 181 lines with 50 m cross-line spacing. Binning and streamer feathering allow 181 lines from the original 81 lines.

General Interpretation

The décollement is easily recognized in our seismic section. It produces a distinctive reflection at the base of the accretionary wedge that is typical of other subduction thrusts (e.g., Barbados; Shipley et al., 1994). Discrete thrusts separate the fold-and-thrust sequences of the accretionary wedge and sole into the high-amplitude décollement reflection, marking it as the basal detachment, parallel to the reflection of subducting ocean crust (Fig. 2A). This area was chosen for the known imaging qualities and because the décollement remains within the relatively homogeneous Lower Shikoku Basin facies (Aoki et al., 1982; Moore et al., 1990), which allows an interpretation that the seismic reflections are predominantly due to porosity changes rather than lithology changes.

The seismic reflection amplitude of the protodécollement increases laterally from minimal to strong across 8 km seaward of the wedge toe. This pattern reveals the regional character and agrees with Ocean Drilling Program (ODP) drilling at specific sites. At ODP Site 1173, 12 km seaward of the wedge toe, drilling recovered a homogeneous hemipelagic sequence of clay and mudstone with minimal physical-property contrasts (Shipboard Scientific Party, 2001). At Site 808, 2 km landward of the deformation front, both velocity and density decrease and porosity increases across a 7 m interface at the base of a 27-m-thick décollement (Fig. 2D). Décolle-

ment seismic reflections have seismic wave polarity opposite the seafloor, consistent with physical property changes at Site 808 (Moore and Shipley, 1993). High porosity beneath the décollement reflection has been attributed to delayed consolidation following rapid loading of the trench turbidites and wedge thickening (Screaton et al., 2002; Saffer and Bekins, 1998).

Between 25 and 40 km landward of the toe, changes occur in the décollement's stratigraphic position. At 25 km (Fig. 2A), the décollement appears to have occasionally stepped down into the underthrust section. The décollement is a continuous weak reflection parallel to the top of the basement (Fig. 2C), and is overlain by an ~250 m layer of discontinuous, subhorizontal reflections (shaded in Fig. 2C). These reflections are distinctly discordant with the overlying steeply dipping strata of the accretionary wedge. The subhorizontal reflections in the shaded sequences continue between discrete thrust sequences and are unbroken by thrusts soling into the décollement. These sequences are underplated sedimentary material attached to the accretionary-wedge base as the décollement stepped down stratigraphic levels. Underplating is identifiable on all of the seismic lines beginning at ~25 km from the trench, but shows along-strike variability (Fig. 2B). Physical property contrasts from differences in the stress histories or lithologies between accreted and underplated sediment could potentially cause the subhorizontal reflections above the décollement. Other similar deep strong reflections (Park et al., 2002) are found in equivalent structural positions on regional seismic profiles.

Between 30 and 40 km (Fig. 2A), there is an abrupt increase in the wedge taper corresponding to the large-thrust sequences identified by Moore et al. (2001a, 2001b). Discrete thrusts separate imbricate sequences and also appear to sole into the décollement; however, these sequences are much thicker and longer than the seaward analogues. At 45 km from the trench, the décollement steps down again through the entire underthrust sequence to near the top of the oceanic basement, underplating all of the remaining underthrust sequence. This downward step of the décollement extends along strike across the entire 8 km width of the three-dimensional survey. The step down to basement merges the décollement and strong basement reflections, making them indistinguishable.

MAP OF DÉCOLLEMENT-REFLECTION AMPLITUDE

The three-dimensional seismic volume gives us an unprecedented look at seismic properties of the fault and their variability across an 8×50 km^2 area. We mapped the décollement amplitudes by digitizing each of the 181 dip lines and comparing them with selected cross lines to assure consistency. We picked the reflection's negative lobe, which was nearly always larger than the positive lobes because of reversed seismic wave polarity. Polarity is straightforward at the deformation front, but is increasingly ambiguous landward of 25 km (Fig. 2A) because of reflection strength and interference. Amplitudes were corrected for spherical divergence, but not for other second-order effects such as attenuation. Consequently, amplitudes are biased to slightly higher values along the shallower, seaward parts of the décollement, but such bias is minimal and not the cause of the large amplitude variability.

High-amplitude décollement reflections at the toe (Fig. 2A) extend along strike, but not downdip. The highest décollement amplitudes (purple areas in Fig. 2B) form within a narrow area along and seaward of the deformation front. Downdip 10–12 km from the toe, the amplitudes level out at values lower by a factor of four to five. Some along-strike amplitude variability exists, which is not due to cross-strike décollement or accretionary wedge structure. Landward of ~12 km (Fig. 2B) the amplitudes become patchy, with high amplitudes remaining to ~25 km, but not farther landward. A second lower amplitude level develops farther downdip (orange areas), which is close to noise levels.

LOSS OF FLUID SOURCES ALONG THE SUBDUCTION THRUST

We propose that the reflection amplitude of the Nankai décollement and its downdip variation are probably largely attributable to differences in pore-fluid content across the décollement. This is supported by the following observations: (1) The lithologic homogeneity of the Lower Shikoku Basin facies (Moore et al., 2001b) within which the décollement forms and propagates is otherwise poorly reflective. There are no reflective stratigraphic horizons into which the décollement can step down. Décollement reflection amplitudes are most likely due to fluids and unlikely affected by minimal lithology changes or changes in décollement stratigraphic level. (2) The décollement reflection has predominantly reversed seismic wave polarity, which has been explained as due to underconsolidation and overpressures within a subduction-zone décollement (e.g., Bangs et al., 1999). Here this condition persists to 30 km landward of the deformation front, beyond which the porosity contrast across the décollement may decrease beneath the thickening prism. Cementation and diagenesis can affect reflectivity, but these processes typically increase velocity and density and thus yield positive polarity, which is generally not seen between 0 and 30 km (Fig. 2A). Landward of 30 km, positive-polarity reflections are not evident, but polarity is more equivocal with these deeper seismic reflections. (3) The décollement reflection waveforms are broadly consistent with reflections from a single interface, which was confirmed by drilling at the wedge toe. The single interface is unlikely a shearing-induced fabric, which typically generates a seismically resolvable shear zone tens of meters thick, a compound seismic reflection, and a positive polarity due to shear-induced clay mineral alignment and consolidation. (4) Reflection amplitudes are sensitive to porosity changes, because seismic amplitudes are a function of the product of velocity and density (seismic impedance), and both positively correlate with decreasing porosity. We tested the sensitivity of the reflectivity to porosity using reflection coefficients derived from these data and empirical relationships of velocity, density, and porosity to relate porosity to reflection coefficient. We estimate that décollement reflections can be seen with porosity contrasts across the décollement as little as ~1%. (5) ODP drilling confirmed that delayed consolidation causes the velocity and density anomalies beneath the décollement at the wedge toe, consistent with observations of reflection amplitude and polarity (Moore et al., 2001b). The reversed-polarity reflections downdip from the ODP drill sites are thus probably also caused by delayed consolidation and potentially excess pore pressure within underthrust sedimentary material.

Consistent with these observations, we speculate that the downdip decrease in reflection amplitude primarily reflects fluid loss from consolidation. Thus, we map the downdip extent of the fluid-rich fault. Estimates of consolidation based on steady-state hydrogeologic models that account for subduction geometry, rates, bulk permeabilities, and fluid sources from dehydration reactions (Saffer and Bekins, 1998), predict that the porosity increase across the décollement at Site 808 gradually disappears by 25–30 km downdip, in excellent agreement with the pattern of declining reflection amplitudes. Hydrogeologic models predict porosity values of ~26% at 12 km and ~10% at 30 km from the trench (Saffer and Bekins, 1998), which are both generally consistent with the seismic amplitudes. There are, however, some along-strike variations, which indicate that this is a diffuse transition spatially and possibly temporally. Thus, the pattern of seismic amplitudes is consistent

with predictions of fluid content from consolidation and dehydration reactions.

If seismic amplitudes are directly related to the fluid content of the fault zone and directly subjacent rocks (within resolvable limits stated above), then our results suggest that excess fluid sources are significantly depleted by ~25 km from the trench. The weak seismic reflections landward of ~25 km preclude the possibility that porosities, and porosity contrasts across the décollement, are large enough for deep sources to reverse the trend of declining fluid content within the fault. The fluid content of the décollement probably continues to decline deeper than 25 km, thus decreasing the potential for excess fluid pressures.

If seismic reflection amplitudes are indicative of porosity contrast across the Nankai subduction thrust, then they could also indicate a loss of excess fluid pressure, following the effective stress concept (Hubbert and Rubey, 1959). As fluid pressures influence the effective stress state acting on the fault zone (Hubbert and Rubey, 1959), a reduction in pore pressure would cause an increase in effective stress, and therefore, an increase in the critical shear stress necessary for slip to occur along the fault. The associated change in fault strength could explain several features: (1) the step down of the décollement if the shallow detachment surface becomes too strong, as others have suggested (e.g., Westbrook and Smith; Saffer, 2003), (2) the increase in wedge taper, according to critical Coulomb wedge theory (e.g., Davis et al., 1983), and (3) a stronger décollement, which would enable greater buildup of elastic strain during interseismic periods, and lead to higher stress drop capable of creating earthquake slip. Loss of excess fluid pressure has been postulated as a significant cause for the aseismic-to-seismic transition at the updip limit of the seismogenic zone (e.g., Moore and Saffer, 2001; Scholz, 1998).

ACKNOWLEDGMENTS

We thank Casey Moore, *Geology* reviewer Julie Morgan, and an anonymous reviewer for very helpful comments and suggestions. We also thank *Geology* editor Ben van der Pluijm. This work was supported by National Science Foundation grant OCE-9730637. University of Texas Institute for Geophysics contribution 1680.

REFERENCES CITED

Ando, M., 1975, Source mechanisms and tectonic significance of historical earthquakes along the Nankai Trough: Tectonophysics, v. 27, p. 119–140.

Ando, M., 1982, A fault model of the 1946 Nankaido earthquake derived from tsunami data: Physics of the Earth and Planetary Interiors, v. 28, p. 320–336.

Aoki, Y., Tamano, T., and Kato, S., 1982, Detailed structure of the Nankai Trough from migrated seismic sections, *in* Watkins, J.S., and Drake, C.L., eds., Studies in continental margin geology: American Association of Petroleum Geologists Memoir 34, p. 309–322.

Bangs, N.L., Shipley, T.H., Moore, J.C., and Moore, G.F., 1999, Fluid accumulation and channeling along the northern Barbados Ridge décollement thrust: Journal of Geophysical Research, v. 104, p. 20,399–20,414.

Byrne, D.E., Davis, D.M., and Sykes, L.R., 1988, Loci and maximum size of thrust earthquakes and the mechanics of the shallow region of subduction zones: Tectonics, v. 7, p. 833–857.

Davis, D., Dahlen, A., and Suppe, J., 1983, Mechanics of fold-and-thrust belts and accretionary wedges: Journal of Geophysical Research, v. 88, p. 1153–1172.

Hubbert, M.K., and Rubey, W., 1959, Role of fluid pressure in mechanics of overthrust faulting: Parts I and II: Geological Society of America Bulletin, v. 70, p. 115–205.

Hyndman, R.D., Wang, K., and Yamano, M., 1995, Thermal constraints on the seismogenic portion of the southwestern Japan subduction thrust: Journal of Geophysical Research, v. 100, p. 15,373–15,392.

Kodaira, S., Takahashi, N., Nakanishi, A., Miura, S., and Kaneda, Y., 2000, Subducted seamount imaged in the rupture zone of the 1946 Nankaido earthquake: Science, v. 289, p. 104–106.

Marone, C., 1998, Laboratory-derived friction laws and their application to seismic faulting: Annual Reviews of Earth and Planetary Sciences, v. 26, p. 643–696.

Moore, J.C., and Saffer, D., 2001, Updip limit of the seismogenic zone beneath the accretionary prism of southwest Japan: An effect of diagenetic to low-grade metamorphic processes and increasing effective stress: Geology, v. 29, p. 183–196.

Moore, G.F., and Shipley, T.H., 1993, Character of the décollement in the ODP Leg 131 area, Nankai Trough, *in* Taira, A., Hill, I.A., et al., Proceedings of the Ocean Drilling Program, Scientific results, Volume 131: College Station, Texas, Ocean Drilling Program, p. 73–82.

Moore, G.F., Shipley, T.H., Stoffa, P.L., Karig, D.E., Taira, A., Kuramoto, S., Tokuyama, H., and Suyehiro, K., 1990, Structure of the Nankai Trough accretionary zone from multichannel seismic reflection data: Journal of Geophysical Research, v. 95, p. 8753–8765.

Moore, G.F., Taira, A., Bangs, N.L., Kuramoto, S., Shipley, T.H., Alex, C.M., Gulick, S.S., Hills, D.J., Ike, T., Ito, S., Leslie, S.C., McCutcheon, A.J., Mochizuki, K., Morita, S., Nakamura, Y., Park, J.O., Taylor, B.L., Toyama, G., Yagi, H., and Zhao, Z., 2001a, Data report: Structural setting of the Leg 190 Muroto transect, *in* Moore, G.F., Taira, A., Klaus, A., et al., Proceedings of the Ocean Drilling Program, Initial reports, Volume 190: College Station, Texas, Ocean Drilling Program, p. 1–14.

Moore, G.F., Taira, A., Klaus, A., Becker, L., Boeckel, B., Cragg, A., Dean, A., Fergusson, C.L., Henry, P., Hirano, S., Hisamitsu, T., Hunze, S., Kastner, M., Maltman, A.J., Morgan, J.K., Murakami, Y., Saffer, D.M., Sánchez-Gómez, M., Screaton, E.J., Smith, D.C., Spivack, A.J., Steurer, J., Tobin, H.J., Ujiie, K., Underwood, M.B., and Wilson, M., 2001b, New insights into deformation and fluid flow processes in the Nankai Trough accretionary prism: Results of Ocean Drilling Program Leg 190: Geochemistry Geophysics Geosystems, v. 2, doi: 10.129/2001GC000166.

Obana, K., Kodaira, S., Kaneda, Y., Mochizuki, K., Shinohara, M., and Suyehiro, K., 2003, Microseismicity at the seaward updip limit of the western Nankai Trough seismogenic zone: Journal of Geophysical Research, v. 108, no. B10, 2459, doi: 10.1029/2002JB002370.

Okino, K., and Kato, Y., 1995, Geomorphological study on a clastic accretionary prism; the Nankai Trough: Island Arc, v. 4, p. 182–198.

Park, J.-O., Tsuru, T., Takahashi, N., Hori, T., Kodaira, S., Nakanishi, A., Miura, S., and Kaneda, Y., 2002, A deep strong reflector in the Nankai accretionary wedge from multichannel seismic data: Implications for underplating and interseismic shear stress release: Journal of Geophysical Research, v. 107, no. B4, 2061, doi: 10.1029/2001JB000262.

Saffer, D.M., 2003, Pore pressure development and progressive dewatering in underthrust sediments at the Costa Rican subduction margin: Comparison with northern Barbados and Nankai: Journal of Geophysical Research, v. 108, no. B5, 2261, doi: 10.1029/2002JB001787.

Saffer, D.M., and Bekins, B.A., 1998, Episodic fluid flow in the Nankai accretionary complex; timescale, geochemistry, flow rates, and fluid budget: Journal of Geophysical Research, v. 103, p. 30,351–30,370.

Scholz, C.H., 1998, Earthquakes and friction laws: Nature, v. 391, p. 37–42.

Screaton, E., Saffer, D., Henry, P., Hunze, S., and Leg 190 Shipboard Scientific Party, 2002, Porosity loss within the underthrust sediments of the Nankai accretionary complex: Implications for overpressures: Geology, v. 30, p. 19–22.

Shipboard Scientific Party, 1991, Site 808, *in* Taira, A., et al., Proceedings of the Ocean Drilling Program, Initial reports, Volume 131: College Station, Texas, Ocean Drilling Program, p. 71–434.

Shipboard Scientific Party, 2001, Site 1173, *in* Moore, G.F., et al., Proceedings of the Ocean Drilling Program, Initial reports, Volume 190: College Station, Texas, Ocean Drilling Program, p. 1–147.

Shipley, T.H., Moore, G.F., Bangs, N.L., Moore, J.C., and Stoffa, P.L., 1994, Seismically inferred dilatancy distribution, northern Barbados Ridge décollement: Implications for fluid migration and fault strength: Geology, v. 22, p. 411–414.

Tanioka, Y., and Satake, K., 2001, Detailed coseismic slip distribution of the 1944 Tonankai earthquake estimated from tsunami waveforms: Geophysical Research Letters, v. 28, p. 1075–1078.

Westbrook, G.K., and Smith, M.J., 1983, Long decollements and mud volcanoes: Evidence from the Barbados Ridge Complex for the role of high pore-fluid pressure in the development of an accretionary complex: Geology, v. 11, p. 279–283.

Manuscript received 1 October 2003
Revised manuscript received 26 December 2003
Manuscript accepted 6 January 2004

Printed in USA

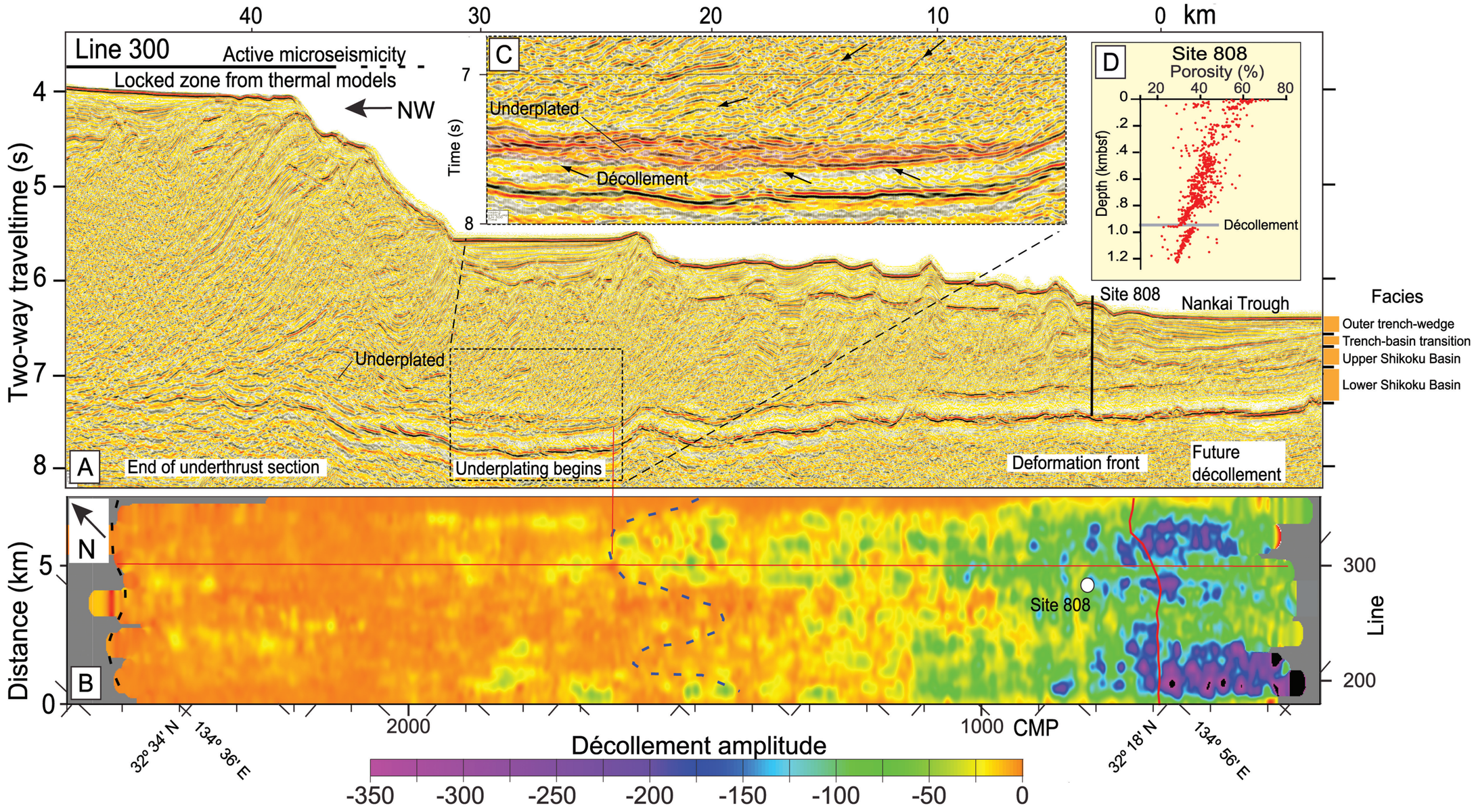

Figure 2. A: Seismic line 300. B: Map of décollement-reflection relative amplitude across 8 × 50 km^2 area of Nankai Trough décollement. Seismic section and map are aligned horizontally and have same horizontal scale. Seismic section is displayed with automatic amplitude gain, whereas map displays actual amplitudes with spherical-divergence corrections. Red line is deformation front. Blue dashed line marks updip edge of underplating. Black dashed line is downdip edge of underthrust section. C: Close-up of seismic line illustrates underplated section (red shading). Up arrows point to décollement. Down arrows show dipping strata within thrust sequences. D: Inset shows porosity across décollement (Shipboard Scientific Party, 1991); kmbsf—km below seafloor. CMP—common midpoint.

Evolution of the Nankai Trough décollement from the trench into the seismogenic zone: Inferences from three-dimensional seismic reflection imaging
Bangs et al.
Figure 2
Supplement to *Geology*, v. 32, no. 4 (April 2004)